critical difference between NMDA and non-NMDA channels, their deactivation kinetics. Rapid removal of glutamate led to a rapid termination of non-NMDA–mediated currents. The ensemble average of currents during this rapid termination can be well fitted to a single exponential. Aniracetam prolonged the deactivation kinetics from 2.9 to 5.7 ms for the patch shown in Fig. 3D.

Desensitization at the macroscopic current level can be due to a number of different mechanisms operating at the microscopic single-channel level. Lectins such as concanavalin A (Con A) and wheat germ agglutinin (WGA) alter non-NMDA desensitization in an irreversible manner (*14, 15*). The lectins and aniracetam differ somewhat in their actions on synaptic currents. Con A does not alter EPSC kinetics (*14*). WGA prolongs the EPSC kinetics but primarily causes a significant increase in amplitudes of the EPSC (*15*). The reasons for these differences are not yet clear.

These data have several implications for the understanding of non-NMDA glutamate channels and synaptic phenomena subserved by them. First, these results and those reported earlier by Ito and co-workers (*7*) show that aniracetam can be used to selectively modulate fast excitatory synaptic currents. Aniracetam can also be effectively used to slow the kinetics of non-NMDA channel so that they can be better resolved. Second, these results have significant implications for hypotheses regarding the mechanisms responsible for the expression of long-term potentiation (LTP). The increase caused by aniracetam in the amplitude of synaptic responses is reduced by almost 50% after induction of LTP (*16*), and the time point in the response at which the drug begins to act is delayed (*17*). Manipulations that enhance release do not cause effects of these kinds (*16, 17*). In light of aniracetam's actions on channel kinetics, the most plausible explanation is that induction of LTP alters the properties of the postsynaptic receptors. Third, these data directly verify for the case of the glutamate-mediated EPSC a generalized form of a hypothesis initially proposed by Magleby and Stevens (*18*). This hypothesis postulates that the time course of EPSCs is determined by the kinetics of the postsynaptic receptors in response to a very brief exposure of the neurotransmitter. In the case of the fast EPSC, however, the validity for the assumption that the neurotransmitter lifetime within the synaptic cleft is much shorter than the duration of the EPSC is unclear (*11, 13*). These data show that, independent of the possible kinetics of neurotransmitter clearance, the time course of the fast EPSC in the mammalian CNS is predominantly determined by the kinetics of the non-NMDA receptor-channel complex.

REFERENCES AND NOTES

1. I. D. Forsythe and G. L. Westbrook, *J. Physiol. (London)* **396**, 515 (1988).
2. G. L. Westbrook and C. E. Jahr, *Sem. Neurosci.* **1**, 103 (1989).
3. C. F. Zorumski, J. Yang, G. D. Fischbach, *Cell. Mol. Neurobiol.* **9**, 95 (1989).
4. S. Hestrin, R. A. Nicoll, D. J. Perkel, P. Sah, *J. Physiol. (London)* **422**, 203 (1990).
5. R. A. J. Lester, J. D. Clements, G. L. Westbrook, C. E. Jahr, *Nature* **346**, 565 (1990).
6. W. Frostl and L. Maitre, *Pharmacopsychiatry* (Suppl.) **22**, 54 (1989).
7. I. Ito, S. Tanabe, A. Kohda, H. Sugiyama, *J. Physiol. (London)* **424**, 533 (1990).
8. External solution contained 1 mM Mg^{2+} and no added glycine. Membrane potential was held at −80 mV. In some experiments MK-801 (10 μM) and APV (500 μM) were added to show that the high-conductance channels were not NMDA channels. We studied fast desensitization kinetics with a fast perfusion system that changed solutions by switching the flow from the two sides of a theta tubing pulled to a gradually tapering opening of 200 μm. Membrane patches were excised to yield outside-out configurations. Synaptic currents were recorded with the whole-cell configuration of the patch clamp technique in both the cultured neurons and the hippocampal slices. Internal pipette solutions are as in (*11*). Single-channel data were acquired with an integrating patch clamp amplifier (Dagan), filtered at 2 kHz, sampled at 4 kHz, and analyzed with PClamp (Axon Instrument).
9. Experiments were performed with the "blind" whole-cell patch clamp technique in hippocampal slices. Slices from young adult rats were maintained in an interface chamber at 35° ± 1°C with the upper surface of the slices exposed to an atmosphere of humidified 95% O_2 and 5% CO_2. Conventional perfusion medium (flow rate, 1 ml/min) was used. Patch clamp pipettes had resistances of 4 to 7 megohms when filled with an intracellular solution composed of the following: 130 mM cesium gluconate, 10 mM KCl, 10 mM Hepes, 2 mM adenosine triphosphate, 0.2 mM guanosine triphosphate, pH = 7.3, 275 mosmol. On approach to a cell, gentle suction was applied to the pipette until a gigaseal was obtained (typically 1 to 10 gigaohms). A holding potential of −70 mV was then applied and the membrane patch ruptured by suction. Typical whole-cell input resistance was 100 to 300 megohms. Synaptic currents were evoked by stimulation of Schaffer commissural afferents with electrodes positioned in the stratum radiatum proximal to the cell body layer. Priming stimulation was used to suppress inhibitory synaptic currents during the responses [J. Larson and G. Lynch, *Science* **232**, 985 (1986)].
10. Neurons were isolated from 20-day-old rat embryos, incubated in Ca^{2+}-free buffer, triturated, and plated in 35-mm tissue dishes that had been coated with a thin layer of Matrigel (Collaborative Research). Cells were maintained in minimum essential medium supplemented with 10% fetal bovine serum and 5% horse serum. Cytosine arabinoside (10 μM) was added when the background glial cell layer became confluent at about 1 week after initial plating.
11. C.-M. Tang, M. Dichter, M. Morad, *Science* **243**, 1474 (1989).
12. P. Ascher and L. Nowak, *J. Physiol. (London)* **399**, 227 (1988).
13. L. O. Trussell and G. D. Fischbach, *Neuron* **3**, 209 (1989).
14. M. L. Mayer and L. Vyklicky, *Proc. Natl. Acad. Sci. U.S.A.* **86**, 1411 (1989).
15. C. F. Zorumski, L. L. Thio, G. D. Clark, D. B. Clifford, *Soc. Neurosci. Abstr.* **16**, 547 (1990).
16. P. Xiao, U. Staubli, M. Kessler, G. Lynch, *Hippocampus*, in press.
17. U. Staubli, J. Ambros-Ingerson, G. Lynch, *ibid.*, in press.
18. K. L. Magleby and C. F. Stevens, *J. Physiol. (London)* **223**, 173 (1972).

19. Supported by a Klingenstein Foundation Award and NIH grant NS28158 (to C.-M.T.) and Air Force Office of Scientific Research grant 890383 (to G.L.). We thank M. Rogawski for helpful suggestions. We thank D. Groul for suggestions that helped with the culturing of cell and G. Clark for the use of Matrigel.

27 June 1991; accepted 27 August 1991

Laser Ablation Studies of the Role of the *Drosophila* Oocyte Nucleus in Pattern Formation

DENISE J. MONTELL, HAIG KESHISHIAN, ALLAN C. SPRADLING

Somatic and germline cells interact during oogenesis to establish the pattern axes of the *Drosophila* eggshell and embryo. The role of the oocyte nucleus in pattern formation was tested with the use of laser ablation. Ablation in stage 6 to 9 egg chambers caused partial or complete ventralization of the eggshell, phenotypes similar to those of eggs produced by *gurken* or *torpedo* females. Accumulation of *vasa* protein at the posterior pole of treated oocytes was also disrupted. Thus the oocyte nucleus is required as late as stage 9 for dorsoventral patterning within the follicle cells and for polar plasm assembly in the oocyte.

THE INITIAL ANTERIOPOSTERIOR and dorsoventral axes and the terminal patterns of the segmented body plan in *Drosophila* are established during oogenesis (*1*). In the ovary, each developing egg chamber contains approximately 1000 somatically derived follicle cells surrounding the 16 germline-derived cells of the oocyte–nurse cell complex (*2*). Communication between the somatic and germline cells contributes to patterning the oocyte (*3*), and also to organizing the eggshell layers produced by the overlying follicle cells (*4*), although exactly where and when developmentally significant information is transferred within egg chambers remains unknown.

D. J. Montell, Carnegie Institution of Washington, Baltimore, MD 21210.
H. Keshishian, Biology Department, Yale University, New Haven, CT 06510.
A. C. Spradling, Howard Hughes Medical Institute and Carnegie Institution of Washington, Baltimore, MD 21210.

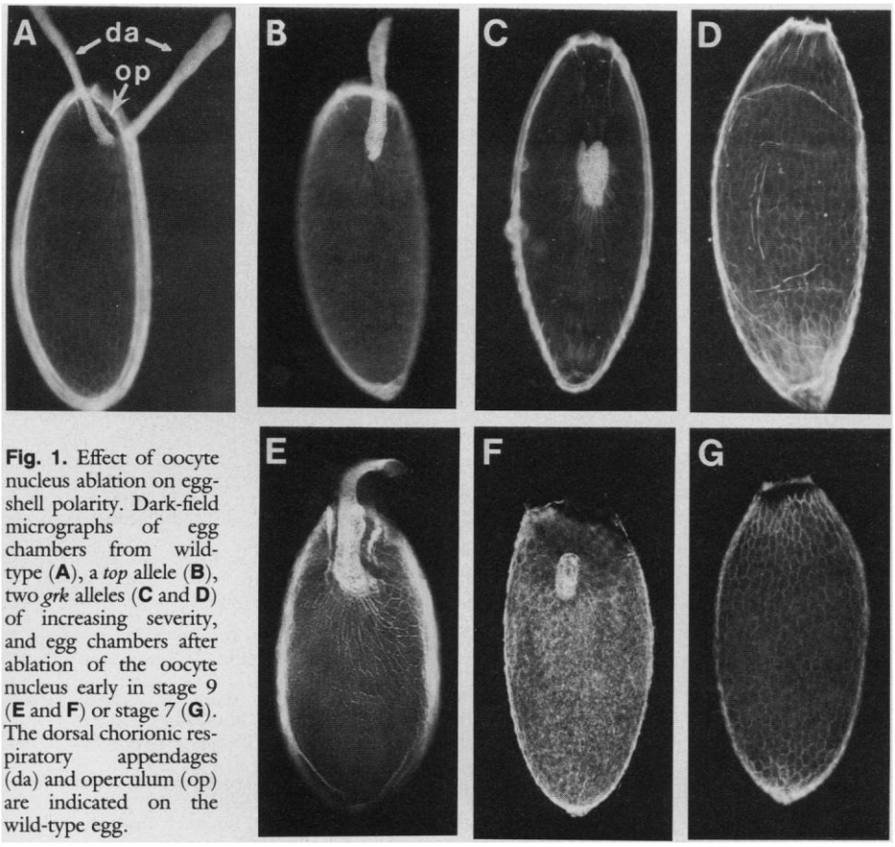

Fig. 1. Effect of oocyte nucleus ablation on eggshell polarity. Dark-field micrographs of egg chambers from wild-type (**A**), a *top* allele (**B**), two *grk* alleles (**C** and **D**) of increasing severity, and egg chambers after ablation of the oocyte nucleus early in stage 9 (**E** and **F**) or stage 7 (**G**). The dorsal chorionic respiratory appendages (da) and operculum (op) are indicated on the wild-type egg.

Table 1. Germinal vesicle ablation; *n*, number.

Structure ablated (*n*)	Ablations attempted (*n*)	Stage 13 or 14 recovered*	
		Normal† (*n*)	Ventralized (*n*)
None	22	9	0
Sham‡	23	17	0
Oocyte nucleus			
Expt. 1§	27	4	2
Expt. 2	60	0	5
Expt. 3	20	5	7
Border cells			
Expt. 1	41	4	0
Expt. 2	50	10	0

*Damage to the delicate egg chambers sometimes occurred during experimental manipulations. This type of damage was less frequent for younger, smaller egg chambers (stage 7 and younger). †In some cases apparently normal egg chambers were recovered even when we had attempted to ablate the oocyte nucleus. Studies of oocyte nuclei marked with β-galactosidase (*12*) revealed that laser treatment frequently, but not always, resulted in the disappearance of the oocyte nucleus. This variation may result from differences in the amount of laser energy delivered to the germinal vesicle depending on the orientation of the mounted egg chambers and the size of the oocyte nucleus. ‡Laser pulses were directed at the cytoplasm in the vicinity of the oocyte nucleus. The site of irradiation was separated from the oocyte nucleus by a distance equal to the diameter of the nucleus. §Experiments are listed separately to illustrate experimental variability.

Signaling within the egg chamber during dorsoventral axis formation has been characterized genetically. Studies of the maternal effect mutants *gurken* (*grk*) and *torpedo* (*top*) led to a model (*5*) in which a germline product is proposed to activate dorsally positioned follicle cells. In the absence of the signal, all follicle cells assume a ventral ground state, resulting in eggs that lack dorsal eggshell structures, and that develop into ventralized embryos. *grk* activity was required in the germline for proper dorsoventral patterning in the follicle cells; however, these experiments did not reveal which of the 16 germline cells carried out this function. A source of the initial dorsalizing signal was suggested (*5*) to be the oocyte nucleus (germinal vesicle), which moves toward the presumptive dorsal surface of the oocyte and subsequently undergoes a period of increased transcriptional activity (*6*).

We tested the postulated role of the germinal vesicle by destroying it with a laser at a time prior to dorsoventral axis formation, and observing the effects on subsequent development. Because the nurse cells provide most of the cytoplasmic components of the *Drosophila* oocyte, ablation of the oocyte nucleus would not be expected to produce a general arrest of oocyte development. Rather, it should only disrupt processes that are initiated within, or at some time require the function of, the oocyte nucleus. In order to bypass the inability of young, isolated egg chambers to develop normally in vitro, egg chambers were injected into the abdomen of a host female for in vivo culture. Such transplanted egg chambers frequently developed to maturity (7). When egg chambers of stages 6 to 9 were mounted in Schneider's medium and selected targets laser-ablated (*8*), egg chambers still developed normally during in vivo culture to stage 14 (Table 1). Egg chambers older than stage 10A were difficult to treat with the laser because of their large size and increased yolk content. One limitation of this approach is that the transplanted egg chambers, developing in the abdomen of the host, could not be fertilized. Thus we could only assess the effects of laser treatment on oocyte development and egg structure, not subsequent embryonic development.

When the oocyte nucleus was irradiated at stages 6 to 9, eggs usually developed with ventralized chorions (Fig. 1) and resembled eggs produced by *top* or *grk* mothers. Dorsal appendage material was reduced or absent, and the operculum region was also missing. Most of the treated eggs were completely ventralized ($n = 12$), resembling those from a strong *grk* allele. In two cases, after stage 9 ablation, partial ventralizations resembling weak and intermediate phenotypes of *grk* and *top* (*5*) were observed (Fig. 1). In one case, ablation of the oocyte nucleus at stage 9 resulted in a completely ventralized chorion. The effect of oocyte nucleus ablation on dorsoventral patterning appeared to be highly specific, as all other visible aspects of oogenesis proceeded normally in germinal vesicle–ablated egg chambers. The oocyte grew to full size, the nurse cells transferred their contents to the oocyte on schedule, and the follicle cells migrated in the manner expected for a ventralized chamber. Eggs resulting from oocyte nucleus ablation did differ from *grk* eggs in that they were not elongated, nor did they have the anterior chorion duplication found at the posterior ends of 30% of *grk* eggs (*3*). The relation of these aspects of the *grk* phenotype to dorsoventral patterning is not clear.

Ventralized chorions were never seen after "sham" ablations in which the oocyte

Table 2. Effect of germinal vesicle ablation on *vasa* localization.

Structure ablated	Ablations attempted (*n*)	Stage 9 or 10A recovered (*n*)	*Vasa* localization	
			Yes (*n*)	No (*n*)
Sham	23	14	14	0
Oocyte nucleus	80	12	4	8

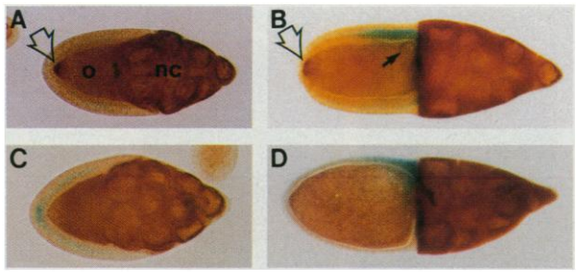

Fig. 2. Effect of oocyte nucleus ablation on posterior *vasa* localization. Nomarski micrographs of normal egg chambers (**A** and **B**) and egg chambers derived from oocyte nucleus ablation experiments (**C** and **D**), stained to indicate dorsal follicle cells (blue, β-galactosidase activity) and *vasa* protein (brown). (A and C) are stage 9 egg chambers; (B and D) are stage 10. The solid arrow indicates the oocyte nucleus. The open arrows indicate localized *vasa* staining at the posterior pole. Note that the specific staining at the posterior poles of the oocytes in (A) and (B) is missing in (C) and (D). The egg chambers were heterozygous for an enhancer trap insertion (PZ8109) that drives expression of β-galactosidase in posterior follicle cells at stage 9 and in dorsal follicle cells from stage 10 to 14. Abbreviations: o, oocyte; nc, nurse cells. Bar represents 60 μm.

cytoplasm was irradiated, or after ablation of the border follicle cells (Table 1). The border cells, a specialized group of six to ten follicle cells, are not expected to participate in dorsoventral pattern formation. We performed ablations at the earliest time these cells were clearly distinguishable (early in stage 9), and consistently recovered egg chambers with normal dorsoventral morphology even in the absence of some or all of the border cells (Table 1).

Studies of the genes *cappuccino* (*capu*) and *spire* (*spir*) suggest that there might be a link between dorsoventral and anteroposterior patterning (*1, 5*). Mutant females produce dorsalized eggs with posterior defects: abnormal abdominal segments, an absence of pole cells, and failure to localize the protein product of the gene *vasa*. *Vasa* encodes a germline-specific protein that is an essential component of the polar plasm and is thought to determine germline cells very early in development (*9*). We tested the effect of oocyte nucleus ablation at stage 6 to 8 on posterior pattern formation by examining *vasa* localization. After irradiation, egg chambers were implanted into host females, dissected at stage 9 or 10A, and stained for *vasa* with the use of an affinity-purified antiserum (Fig. 2 and Table 2). Laser treatment did not affect *vasa* staining in the nurse cells or transfer of cytoplasmic components to the oocyte. However, the accumulation of *vasa* at the posterior pole of the oocyte was frequently reduced or missing. Laser irradiation of the oocyte cytoplasm did not affect posterior *vasa* accumulation.

These experiments support the proposal that the oocyte nucleus is the source of a dorsalizing signal to follicle cells. The signal might be the product of a gene expressed in the germinal vesicle, which, if only able to diffuse over a limited distance, would activate receptors on dorsal but not ventral follicle cells. Germline-dependent genes such as *gurken* and *cornichon* (*10*) may encode such a signal. Alternatively, the oocyte nucleus might be required to assemble or activate a signal originating in the nurse cells. For example, the oocyte nucleus might organize a transport system used to move signal molecules in a polar fashion. Neither model implies that the oocyte nucleus is a primary determinant of dorsoventral polarity; polarity may already exist within the oocyte when the germinal vesicle migrates dorsally.

Our experiments indicate that some and possibly all dorsalizing information is transmitted during or after stage 9, after the oocyte nucleus migrates to the dorsal surface, possibly during its period of transcriptional activity. Had signaling been completed earlier, ablation of the oocyte nucleus in stage 9 egg chambers would not have produced completely ventralized eggshells. The two partial ventralizations following stage 9 ablations probably resulted from incomplete inactivation of the larger stage 9 oocyte nucleus by the laser.

The germinal vesicle also appears to be required for the normal assembly of posterior pole plasm, as indicated by the accumulation of *vasa* protein at the posterior pole of the oocyte. The oocyte nucleus may be required for transcription of posterior group genes, such as *oskar* and *staufen*, as mutations in these genes prevent *vasa* protein accumulation at the posterior pole (*11*). Alternatively, the nucleus may be part of a cytoskeletal network that is required for transport of determinants within the oocyte.

The effects of germinal vesicle ablation might derive from reductions in both transcription and transport. If *capu* and *spir* protein products localize both a dorsalizing signal originating in the oocyte nucleus as well as *vasa* protein produced by the nurse cells, failure to localize the nucleus-derived determinant specifically to the dorsal side could result in dorsalization similar to that seen in *capu* and *spir* mutants. Absence of the oocyte nucleus, and thus of the determinant, would cause ventralization of the egg, like that seen in double mutants of *capu* or *spir* in combination with *grk*. Further insights into the nature of the protein products encoded by the posterior group genes and their expression patterns as well as molecular analysis of the *capu* and *spir* loci should aid in distinguishing these possibilities.

Laser ablation can supplement genetic mosaic analysis in determining the functions of specific egg chamber cells and the timing of developmental events. Although this approach is limited by the inability to assess subsequent embryonic development, laser ablation can contribute to our understanding of the organization and development of the unfertilized egg.

REFERENCES AND NOTES

1. L. Manseau and T. Schupbach, *Trends Genet.* **5**, 400 (1989).
2. A. Mahowald and R. Kambysellis, in *The Genetics and Biology of* Drosophila, M. Ashburner and T. Wright, Eds. (Academic Press, New York, 1980), vol. 2d, p. 141.
3. T. Schupbach, *Cell* **49**, 699 (1987); L. Stevens, L. Fronhoffer, C. Nüsslein-Volhard *Nature* **335**, 275 (1990).
4. E. Wieschaus, J. Marsh, W. Gehring, *Wilhelm Roux's Arch. Dev. Biol.* **184**, 75 (1978).
5. L. Manseau and T. Schupbach, *Genes Dev.* **3**, 1437 (1989).
6. A. P. Mahowald and M. Tiefert, *Wilhelm Roux's Arch. Dev. Biol.* **165**, 8 (1970).
7. H. Gutzeit and R. Koppa, *J. Embryol. Exp. Morphol.* **67**, 101 (1982).
8. Laser ablations were performed as follows: after dissection in Schneider's medium [I. Schneider, *ibid.* **27**, 353 (1972)] supplemented with 10% fetal calf serum, egg chambers were mounted on slides. Egg chambers were obtained from either Canton-S *Drosophila melanogaster* females or from females heterozygous for one of three enhancer trap lines [C. O'Kane and W. Gehring, *Proc. Natl. Acad. Sci. U.S.A.* **84**, 9123 (1987)]. Lines PZ258, PZ8109, and PZ107 each contain a single PZ element insertion [M. Mlodzik, Y. Hiromi, U. Weber, C. Goodman, G. Rubin, *Cell* **60**, 211 (1990)] that drives β-galactosidase expression in the border cells, dorsal follicle cells, or germline cells, respectively. Cover slips were supported by dabs of vacuum grease that allowed the egg chambers to be compressed just enough to prevent them from moving. Egg chambers were oriented at random under the cover slip with respect to their future dorsoventral axis. Ablations were performed with the use of a VSL 337 nitrogen laser driving a mirror-to-mirror dye module (Laser Sciences Inc., Cambridge, MA) of 3-nsec duration and peak power of 5 to 8 kilowatts. Coumarin 440 was the laser dye. The pulses were focused with a 75-mm planoconvex lens and reflected into the epiillumination optical train of a Zeiss 4FL fluorescence microscope, with the use of a 510-nm dichroic mirror. The illuminated area was a 2 by 1 μm ellipse. The laser was fired as a burst of ten shots spaced over 1 s. Two to ten successive bursts were used. The egg chamber was then recovered from the slide, injected into the abdomen of an Fs(1) ovo^{D1} female (*7*), cultured in vivo for 1 or 2 days at 22°C or 25°C depending on the stage injected and the stage required for analysis, and recovered by dissection.
9. B. L. Hay, S. Ackerman, S. Barbel, L. Jan, Y. Jan, *Development* **103**, 625 (1988); P. Lasko and M. Ashburner, *Nature* **335**, 611 (1988); B. Hay, L. Jan, Y. Jan, *Development* **109**, 425 (1990); P. Lasko and M. Ashburner (*11*).
10. M. Ashburner *et al.*, *Genetics* **126**, 679 (1990).
11. P. Lasko and M. Ashburner, *Genes Dev.* **4**, 905 (1990).
12. Enhancer trap line PZ107 was used in some ablation experiments to study the survival of the oocyte nucleus. This strain expresses β-galactosidase activity in

the nurse cells and oocyte nucleus throughout oogenesis. To determine the fate of germinal vesicles after ablation, PZ107 egg chambers were recovered from host females at various times after ablation, fixed, and stained for β-galactosidase activity. In some egg chambers (n = 7), the oocyte nucleus was absent based on β-galactosidase staining, whereas in other egg chambers (n = 4) a stained nucleus remained. In four cases, β-galactosidase and *vasa* localization were examined in the same egg chamber after germinal vesicle ablation. In two of these cases, both were absent; in one case, the oocyte nucleus failed to stain for β-galactosidase and yet *vasa* protein was still localized apparently normally. In the fourth case, a β-galactosidase–positive oocyte nucleus was found even though *vasa* protein was not localized. This may indicate that there are multiple aspects of oocyte nucleus function which can be eliminated separately or in concert.

13. We thank L. Cooley for encouragement and facilities, P. Lasko and M. Ashburner for the *vasa* antibody, T. Schüpbach for advice, E. Hersperger and A. Simcox for instruction concerning egg chamber injection into hosts, and A. Fine and the Rita Allen Foundation for laser and microscope facilities. Supported by a postdoctoral fellowship to D.J.M. and by grants from the March of Dimes and NIH to H.K.

10 April 1991; accepted 23 July 1991

Suppression of Tumorigenicity in Wilms Tumor by the p15.5-p14 Region of Chromosome 11

STEVEN F. DOWDY,* CLARE L. FASCHING, DIANA ARAUJO, KIN-MAN LAI, ELIZABETH LIVANOS, BERNARD E. WEISSMAN, ERIC J. STANBRIDGE†

Wilms tumor has been associated with genomic alterations at both the 11p13 and 11p15 regions. To differentiate between the involvement of these two loci, a chromosome 11 was constructed that had one or the other region deleted, and this chromosome was introduced into the tumorigenic Wilms tumor cell line G401. When assayed for tumor-forming activity in nude mice, the 11p13-deleted, but not the 11p15.5-p14.1–deleted chromosome, retained its ability to suppress tumor formation. These results provide in vivo functional evidence for the existence of a second genetic locus (WT2) involved in suppressing the tumorigenic phenotype of Wilms tumor.

WILMS TUMOR, A PEDIATRIC NEPHROBLASTOMA, originates from embryonal kidney stem cells and presents itself in either a classical form or a differentiated form (*1*). The classical form comprises embryonic blastema cells, whereas the differentiated form may contain a variety of cell types, including striated muscle, squamous epithelial, and cartilaginous cells. Wilms tumor occurs in either a familial or sporadic form; >95% of all Wilms tumors are of the sporadic form (*2*). Cytogenetic analysis of Wilms tumors from patients with the familial WAGR syndrome (Wilms tumor, aniridia, genital urinary abnormalities, and mental retardation) shows interstitial deletions of chromosome 11 that include 11p13 (*3*). Restriction fragment length polymorphism (RFLP) analysis revealed a loss of heterozygosity (LOH) of surrounding DNA markers in the 11p13 region from some sporadic Wilms tumors (*4*). Thus, the region may encode a tumor suppressor gene, the inactivation of which is required for progression to the malignant state. A candidate 11p13 Wilms tumor suppressor gene cDNA, named WT1, was isolated and is specifically expressed during normal kidney development (*5, 6*). However, RFLP analyses of sporadic Wilms tumors have also indicated a LOH of DNA markers in the 11p15 region, named WT2 (*7*), in the absence of any detectable alteration in the 11p13 region, suggesting the involvement of a second genetic locus in the etiology of Wilms tumor (*8*). In addition, two reports have excluded the involvement of both the 11p13 region and the 11p15 region in some familial Wilms tumors (*9*), suggesting the involvement of a third genetic locus.

We have investigated the regions of chromosome 11 that may contribute to suppression of the tumorigenic phenotype in the G401 Wilms tumor cell line. Copies of chromosome 11, with appropriate deletions, were transferred into G401 cells by the microcell-mediated chromosome transfer (MMCT) technique (*10*). The G401 cell line, isolated directly from an explant of a Wilms tumor from a 3-month-old male (*11*), is undifferentiated in culture, which is consistent with the establishment of other Wilms tumor cell lines (*12*). It is pseudodiploid with a single marker 12 chromosome and contains no cytogenetically detectable deletion or alteration of either chromosome 11 homolog. G401 is immortal in vitro and forms tumors when injected subcutaneously into nude mice. When a balanced X;11 translocated human chromosome [der(11)t(X;11)(q26;q23)] that contains >90% of chromosome 11 is introduced into G401.6TG.6 (HPRT-clone of G401) cells by MMCT, the tumorigenic potential of G401 cells is suppressed, whereas the introduction of "irrelevant" X and X;13 [der(13)t(X;13)(p22;q12)] chromosomes does not affect tumorigenesis (*13*). To further define the region that contains the tumor suppressor information for the G401 Wilms tumor cell line, we transferred a naturally occurring balanced X;11p translocated chromosome [der(11)t(X;11p)-(q21;q13)] from the human fibroblast cell line GM3322 into mouse A9 cells by MMCT, which produced monochromosome hybrid MCH 701.8. The X;11p chromosome was then transferred from MCH 701.8 into G401.6TG.6 cells. The human X;11p chromosome has been characterized cytogenetically and with 17 DNA markers that span the 11p chromosomal arm (*14*) (Fig. 1). The introduction of the X;11p chromosome into G401.6TG.6 resulted in the isolation of two microcell hybrids, MCH 706.1 and MCH 706.2, that contained 47 chromosomes and that were nontumorigenic when inoculated subcutaneously into athymic nude mice (Table 1). The spontaneous segregants of the X;11p chromosome from the nontumorigenic microcell hybrids were selected with the addition of 6-thioguanine to the medium. A segregant thus isolated, MCH 706.2.6TG, contained 46 chromosomes and reexpressed the malignant phenotype (Table 1). This constitutes further evidence of the specific correlation of suppression of tumorigenicity with the presence of normal genetic information on chromosome 11. These results define the region responsible for suppressing the tumorigenic phenotype of the G401 Wilms tumor to 11pter-q13 with an in vivo functional assay.

The introduction of the X;11p chromosome into G401.6TG.6 further localized the tumor suppressor gene but did not differentiate between the 11p13 and 11p15 regions or investigate cooperativity between the two loci. We therefore devised a procedure to enrich for deletion or rearrangement of a specific chromosomal arm (*14*). Two useful radiation-reduced microcell hybrids (XMCH 708.24 and XMCH 708.20) were generated by this method from MCH 701.8 (Fig. 1). The deleted X;11p chromosome present in XMCH 708.24 contained a simple interstitial deletion encompassing the p15.5::p14.1 region and retained an intact 11p13 region. The deleted X;11p chromosome present in XMCH 708.20 contained a

S. F. Dowdy, C. L. Fasching, D. Araujo, K.-M. Lai, E. J. Stanbridge, Department of Microbiology and Molecular Genetics, University of California, Irvine, CA 92717.
E. Livanos and B. E. Weissman, Lineberger Cancer Research Center, University of North Carolina, Chapel Hill, NC 27599.

*Present address: Whitehead Institute, 9 Cambridge Center, Cambridge, MA 02142.
†To whom correspondence should be addressed.